Bioorganic & Medicinal Chemistry 28 (2020) 115423

Contents lists available at ScienceDirect

Bioorganic & Medicinal Chemistry

journal homepage: www.elsevier.com/locate/bmc

Synthesis and biological evaluation of new antioxidant and antiproliferative chalcogenobiotin derivatives for bladder carcinoma treatment

Andrielli Leitemberger[a,1], Mariana S. Sonego[c,1], Fábio D. Garcia[a], Alana C.F. dos Santos[a], Bruna C. Piccoli[b], Fernanda D. da Silva[b], Cláudia S. Oliveira[b], Fabiana K. Seixas[c], Luciano Dornelles[a], João B.T. Rocha[b], Pablo A. Nogara[b], Kyle M. Schachtschneider[d,e,f], Tiago Collares[c], Oscar E.D. Rodrigues[a,*]

[a] LabSelen-NanoBio – Departamento de Química, Universidade Federal de Santa Maria, Santa Maria, Brazil
[b] Laboratório de Bioquímica Toxicológica – Departamento de Bioquímica e Biologia Molecular, Universidade Federal de Santa Maria, Santa Maria, Brazil
[c] Laboratório de Biotecnologia do Câncer, Programa de Pós-Graduação em Biotecnologia (PPGB), Centro de Desenvolvimento Tecnológico (CDTec), Universidade Federal de Pelotas, Campus Universitário s/n, Capão do Leão, RS Cep 96010-900, Brazil
[d] Department of Radiology, University of Illinois at Chicago, Chicago, IL, United States
[e] Department of Biochemistry & Molecular Genetics, University of Illinois at Chicago, Chicago, IL, United States
[f] National Center for Supercomputing Applications, University of Illinois at Urbana-Champaign, Urbana, IL, United States

ARTICLE INFO

Keywords:
Antioxidants
Antiproliferative activity
Biological activity
Biotin
Chalcogen-vitamins

ABSTRACT

Approximately 90% of bladder carcinomas are of the urothelial carcinoma type, which are characterized by high rates of recurrence and predisposition to progress to invasive tumors, representing one of the most costly neoplasms for health systems. Intravesical chemotherapy is a standard for the treatment of non-invasive bladder cancer. However, chemotherapy is usually aggressive and cytotoxic, which increases the death rates caused by cancer. Heterocyclic compounds which exhibit favorable pharmacokinetic and pharmacodynamic properties may enhance drug affinity for a target protein by targeting the treatment. Thus, this work presents the synthesis, characterization, and *in vitro* biological evaluation of new antioxidant (inhibition of lipid peroxidation, scavenging of free radical DPPH, and thiol peroxidase-like activity) and antiproliferative chalcogenobiotin derivatives and tests them against bladder carcinoma 5637 cells. A prominent response was obtained for the selected compounds, with tellurium biotin derivatives displaying effective antioxidant and antiproliferative activity. The effective compounds also demonstrated no toxicity in *in vitro* or *in vivo* studies.

1. Introduction

Organochalcogenium compounds are an important class of organic compounds. The introduction of sulfur, selenium, or tellurium to organic substrates allows for modulation of the properties of these molecules, facilitating application in a variety of fields including organic synthesis, asymmetric catalysts for enantioselective reactions,[1] and key intermediates in organic transformations.[2] In material science, organochalcogenium compounds display liquid crystal properties,[3] and some selenium nanostructures show potential for electronic applications.[4] From a biological perspective, molecules containing chalcogenium display a range of antiviral,[5] antimicrobial,[6] anti-inflammatory,[7] antioxidant,[8] and antitumoral activities.[9] In addition, previous studies have been demonstrated that organochalcogenium compounds can induce tumor cell death, where the modulation of protein kinase pathways could be involved. However, the specific protein target is not known yet.[10–14] Recently, our research group published results demonstrating the antitumoral activity of chalcogenozidovudine derivatives.[15,16] These compounds presented prominent action against bladder carcinoma 5637 cells. Bladder tumor carcinoma is highly prevalent and demonstrates exorbitant costs to public coffers in all regions of the world. The drugs currently used have high toxicity

Abbreviations: DPPH, 2,2-diphenyl-1-picrylhydrazyl; DBU, 1,8-diazabicyclo(5.4.0)undec-7-ene; MTT, 3-(4,5-dimethylthiazol-2-yl)-2,5-diphenyltetrazolium bromide); TBARS, thiobarbituric acid reactive substances; BHT, 2,6-bis(1,1-dimethylethyl)-4-methylphenol; AST, aspartate aminotransferase; ALT, alanine aminotransferase

* Corresponding author.
E-mail addresses: rodriguesoed@gmail.com, rodriguesoed@smail.ufsm.br (O.E.D. Rodrigues).
[1] These authors contributed equally to this work.

https://doi.org/10.1016/j.bmc.2020.115423
Received 23 October 2019; Received in revised form 24 February 2020; Accepted 9 March 2020
Available online 16 March 2020

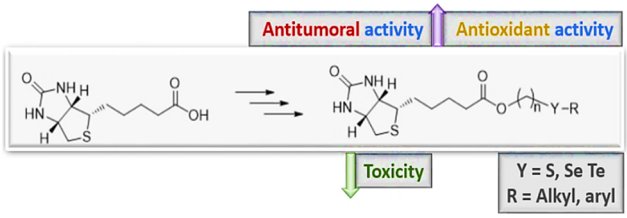

Fig. 1. Synthesis and biological evaluation of chalcogenobiotin derivatives.

and low selectivity, and studies have been done to enhance the action of drugs, improving patient outcomes; including pharmacokinetic techniques to maximize drug delivery and strategies to improve drug absorption and action.[17,18] In this context the search for drugs with selective action against a specific biological target is a prominent research field. This specificity may enhance therapeutic actions and, at the same time, reduce the number of side effects associated with treatments. Antitumor targeting can be specified based on pH levels in antitumor tissue,[19] or overexpression of various receptors on cancerous cells. In this context, the use of biotin as a vector agent for cancer cells can improve targeted delivery due to increased dependence on vitamins and elevated levels of biotin receptors in tumor tissues compared to healthy cells.[20–22] Therefore, this study developed a small library of chalcogenobiotin derivatives from commercially available biotin using a two reaction approach. The antioxidant and antiproliferative activity of the resulting agents was explored using the bladder carcinoma 5637 cell line (Fig. 1).

2. Results and discussion

Chalcogenobiotin derivatives **5a(a-g)** and **5b(a-g)** were synthesized from commercially available biotin utilizing two reactional steps for all derivatives, as depicted in Scheme 1. Following optimization of the reaction conditions, a variety of dichalcogenides were employed in order to prepare a small library of chalcogenobiotin derivatives **5a(a-g)** and **5b(a-g)**.

As observed in Table 1, the respective chalcogenobiotin derivatives were obtained with yields ranging from 66% to 93%. In terms of electronic effects, the reactions were sensitive to the substituents attached to the aryl ring in chalcogenium moiety. For instance, higher yields were obtained by activating groups present in the original dichalcogenides, and a slight decrease in the efficiency was observed for the products containing deactivating groups (Table 1, Entries 2, 3, 4 and 9, 10, 11, respectively). This may be related to the higher nucleophilicity of the chalcogenolates containing activating groups. Additionally, yields for selenium counterparts were higher than sulfur or tellurium derivatives. These results may be related to the lower nucleophilicity of sulfur compared to selenium nucleophiles and the lower stability of tellurolates, due to its higher tendency for oxidation. Furthermore, two alkyl derivatives were also obtained (Entries 5 and 12), showing the versatility of the methodology.

2.1. Antioxidant activity

Reactive oxygen species (ROS) are by-products of aerobic metabolism and could damage proteins, lipids, and DNA. ROS oxidize the DNA, causing mutations that could reflect in cancer initiation.[23] A serious drawback to the development and application of drugs for some therapies - especially antitumoral compounds - is their toxicity, particularly those related to oxidative stress. On the other hand, compounds

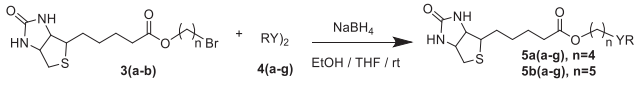

Scheme 1. Synthesis of chalcogenobiotin derivatives **5a(a-g)** and **5b(a-g)**.

Table 1
General scheme for the synthesis of chalcogenobiotin derivatives **5a (a-g)** and **5b (a-g)**, for **Y = Se, Te or S**.

Entry	Cmpd	Y	Product	Yield (%)[a]
1	**5aa**	Se	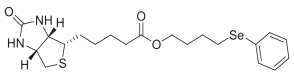	90
2	**5ab**	Se	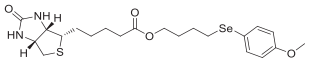	82
3	**5ac**	Se	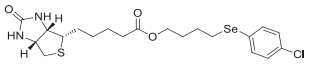	73
4	**5ad**	Se	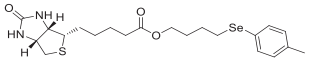	81
5	**5ae**	Se	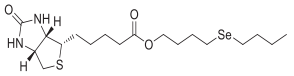	78
6	**5af**	Te	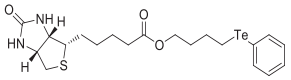	66
7	**5ag**	S	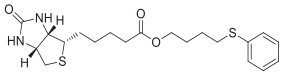	76
8	**5ba**	Se	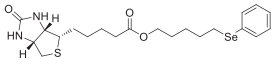	92
9	**5bb**	Se	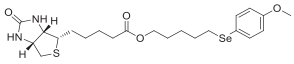	93
10	**5bc**	Se	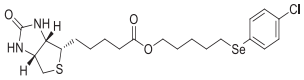	80
11	**5bd**	Se	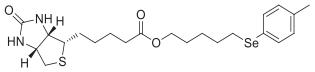	92
12	**5be**	Se	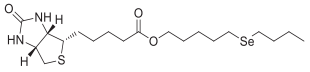	78
13	**5bf**	Te	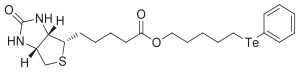	68
14	**5bg**	S	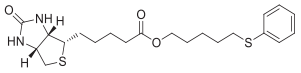	79

[a] Yields refer to the products after purification.

containing chalcogenium, especially selenium and tellurium, appear as efficient protective antioxidants. As such, the chalcogenobiotin derivatives **5af** and **5bf** that displayed antiproliferative activity against 5637 bladder cancer cells (see below) were selected for *in vitro* evaluation as antioxidant agents.

2.2. Scavenger activity of radical 2,2-diphenylpicrylhydrazyl (DPPH)

One of the ways to test the antioxidant effect is by scavenging free radicals.[24] Here, 2,2-diphenyl-1-picrylhydrazyl (DPPH) was used as a free radical to test the ability of compounds **5af** and **5bf** to scavenge it. Dimethyl sulfoxide (DMSO) was used as a vehicle to dissolve the compounds. At 1 mM, compounds **5af** and **5bf** scavenged, approximately 50% of the DPPH (Fig. 2). The time required to scavenge 50% ($t_{1/2}$) of the DPPH radical was calculated using a final concentration of 500 μM, with the compounds presenting a $t_{1/2}$ statistically equal to Butylated Hydroxy Toluene (BHT - positive control) at the same concentration (Table 2).

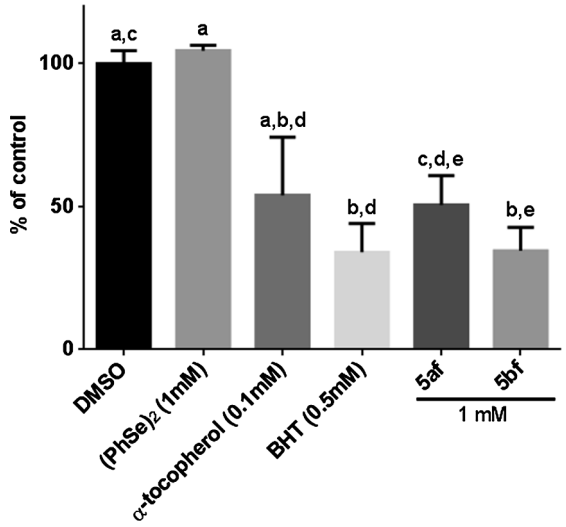

Fig. 2. DPPH scavenging activity induced by chalcogenobiotin derivative compounds (1 mM). ($(PhSe)_2$), butylated hydroxytoluene (BHT, 0.5 mM), and α-tocopherol (0.1 mM) were used as positive controls. Data were expressed as means ± S.E.M. from three independent experiments, and differences are considered significant at $p < 0.05$. Different letters indicated the differences between the compounds (post hoc test: Tukey $p < 0.05$).

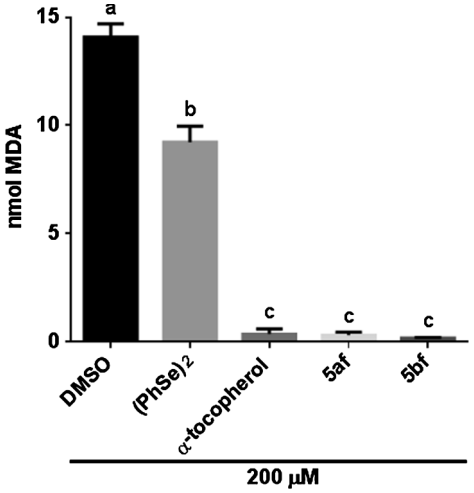

Fig. 3. Effect of the chalcogenobiotin derivative compounds (200 μM) on lipid peroxidation induced by iron. Diphenyl diselenide ($(PhSe)_2$) and α-tocopherol (200 μM) were used as positive controls. Data were expressed as means ± S.E.M. from three independent experiments, and differences are considered significant at $p < 0.05$. Different letters indicated the differences between the compounds (post hoc test: Tukey $p < 0.05$).

Table 2
IC_{50} values for inhibition of lipid peroxidation and $t_{1/2}$ to scavenge DPPH and GPx-like.

Compound	TBARS IC_{50} (μM)	DPPH $t_{1/2}$ (min)	GPx-like t_{50} (min)
$(PhSe)_2$	248.30 ± 9.28[a]	> 180	120.5 ± 27.62[a]
Ebselen	n.d.	n.d.	55.99 ± 6.86[b]
α-tocopherol	60.33 ± 15.94[b]	n.d.	n.d.
BHT	n.d.	20.67 ± 7.22[a]	n.d.
5af	5.00 ± 1.00[c]	18.00 ± 3.00[a]	15.78 ± 0.93[b]
5bf	1.33 ± 0.33[c]	23.00 ± 1.53 [a]	38.86 ± 0.66[b]

n.d.: not determined. Different letters mean significant difference among the compounds (post hoc test: Tukey $p < 0.05$).

2.3. Thiobarbituric acid reactive substances (TBARS)

Oxidative stress also leads to cell injury by lipid peroxidation of cellular membranes.[25] The cellular membrane has mainly phospholipids in its composition. Lipids undergo peroxidation and form aldehydes, such as malondialdehyde.[26] The products of lipid peroxidation react with thiobarbituric acid forming a pink-colored complex that can be quantified in TBARS assay.[27] The antioxidant capacity of chalcogenobiotin derivative compounds was evaluated. All compounds (final concentration 200 μM) inhibited phosphatidylcholine (lipid source) peroxidation induced by Fe(II) (Fig. 3). The compounds **5af** and **5bf** were more effective than one of the positive controls (200 μM diphenyl diselenide) and presented antioxidant activity statistically equal to α-tocopherol (positive control). Inhibitory concentration curves were then calculated. The calculated IC_{50} for lipid peroxidation inhibition was about 5 μM (**5af**) and 1 μM (**5bf**) (Table 2). The IC_{50} values were lower than those found for diphenyl diselenide (248 μM). Nevertheless, compounds **5af** and **5bf** presented IC_{50} values statistically equal to those obtained with α-tocopherol (60 μM). These results indicated that these compounds are effective in preventing lipid peroxidation even at low concentrations.

2.4. Thiol peroxidase-like activity

Glutathione peroxidase (GPx) is an enzyme that belongs to the antioxidant system which converts H_2O_2 (ROS) into H_2O and O_2. Some compounds such as diphenyl diselenide and ebselen can mimic the activity of this enzyme *in vitro*.[28,29] This methodology demonstrates the efficacy of chalcogenobiotin derivatives in mimicking the antioxidant enzyme glutathione peroxidase (GPx), which transforms hydrogen peroxide into water. Compounds **5af** and **5bf** efficiently decomposed H_2O_2 at high concentrations (450 μM), similar to the rate of positive control $(PhSe)_2$ (Fig. 4). When a low concentration was tested (55 μM), compounds **5af** and **5bf** presented a $t_{1/2}$ statistically equal to the positive control Ebselen and lower than diphenyl diselenide at the same concentration (Table 2).

Through these analyses, it is possible to indicate that compounds **5af** and **5bf** have antioxidant activity in three different ways, such as they can scavenge free radicals, protect lipid peroxidation and even mimic the GPx enzyme.

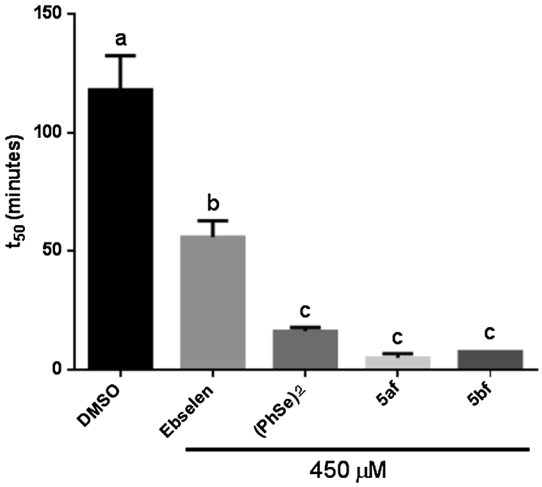

Fig. 4. Thiol peroxidase-like activities with chalcogenobiotin derivatives (450 μM). Diphenyl diselenide ($(PhSe)_2$) was used as the positive control. Data are expressed as means ± S.E.M. from three independent experiments, and differences are considered significant at $p < 0.05$. Different letters indicated the differences between the compounds (post hoc test: Tukey $p < 0.05$).

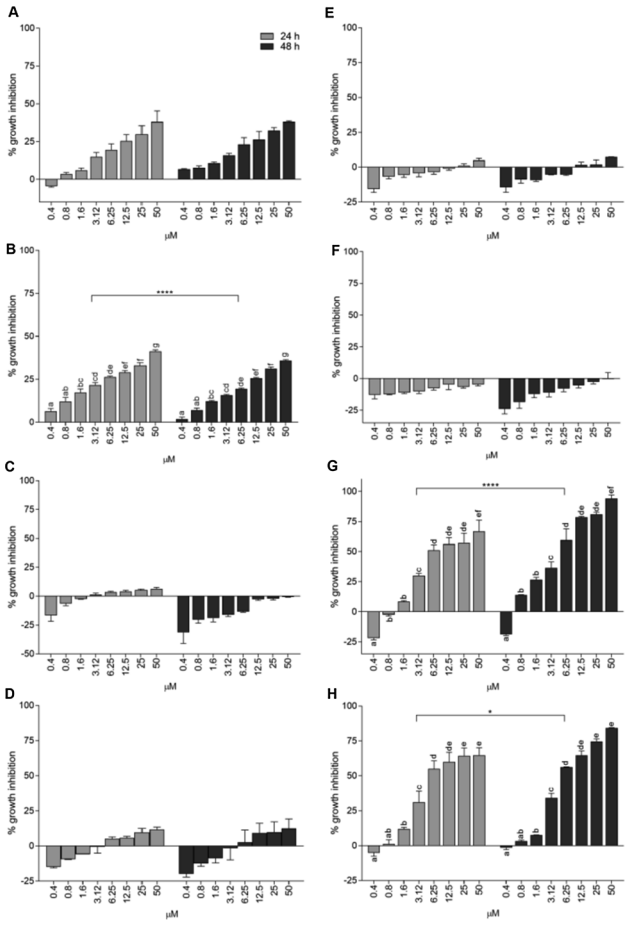

Fig. 5. Antiproliferative effect of Chalcogenobiotin derivatives investigated by MTT assay. Growth inhibition of 5637 cancer cells following exposure to biotin (A), heptyl(phenyl)tellane (B), 5aa (C), 5ab (D), 5ac (E), 5ad (F), 5af (G) and 5bf (H) for 24 and 48 h. Data are expressed as means ± SEM from three independent experiments. The letters indicate the differences between concentrations within each time. Each letter corresponds to a concentration (e.g. 0.4 μM–letter a). * $p = 0.0222$, **** $p < 0.0001$ correspond to the difference between times 24 and 48 h in graphs H and G, respectively.

2.5. Antitumoral activity

It is known that cells need vitamins to survive. Thus, tumor cells with increased metabolic activity have higher requirements for essential vitamins.[30] Biotin is an exogenous vitamin necessary for cellular functions and growth, and its uptake by mammalian cells is mediated by biotin receptors. These receptors display increased expression in tumor cells in order to facilitate greater vitamin uptake.[31]

The cytotoxicity of biotin, **5aa**-**5ad**, **5af**, and **5bf** derivatives was tested by exposing 5637 cell lines to 0.4 to 50 μM of each compound for 24 and 48 h (Fig. 5A, C–H). DMSO (0.5%) was used as a vehicle for drug dilution, and non-treated cells were used as negative controls. Results are shown in Table 3 and Fig. 5.

As observed in Fig. 5A, biotin did not display cytotoxicity in all evaluated concentrations. Selenium derivatives **5aa**, **5ab**, **5ac,** and **5ad** caused no cytotoxicity against the evaluated tumor cells despite the variation of the substituent in the aromatic ring attached to the selenium atom (Fig. 5C–F). Nevertheless, when selenium was modified for tellurium in compounds **5af** and **5bf**, variation in the antiproliferative activity of the chalcogenobiotin derivatives was observed, demonstrating a potent action against 5637 cells at lower concentrations (Fig. 5G, H).

To study the influence of biotin on the antitumoral activity of the tellurobiotin derivatives, we prepared heptyl(phenyl)tellane, a compound containing tellurophenyl attached to an alkylic chain (Fig. 6; for the experimental procedure, see SI file).

Table 3
Susceptibility of Bladder Carcinoma 5637 cells to chalcogenobiotin derivatives.[a]

Compound	IC_{50} 24 h	IC_{50} 48 h
5af	5.8 ± 3.11	4.73 ± 2.13
5bf	7.63 ± 3.17	6.71 ± 1.87
Heptyl(phenyl)tellane	–	–

[a] IC_{50} values are given in μM. All data were obtained from three independent experiments and are presented as mean ± SEM inhibition. It was not possible to calculate the IC_{50} for heptyl(phenyl)tellane, as this compound failed to inhibit 50% of cell growth.

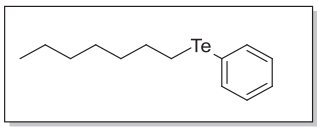

Fig. 6. Heptyl(phenyl)tellane.

Like biotin, heptyl(phenyl)tellane displayed low cytotoxicity (Fig. 5B), which reduced over time. This result demonstrates the importance of biotin-conjugated with the phenyltellurium group for improving antitumoral activity. In addition, the tellurium biotin derivatives **5af** and **5bf** significantly reduced 5637 cell line viability *in vitro* in a time-dose-dependent manner (Fig. 5G and H), while biotin derivatives containing selenium (**5aa**-**5ad**) did not cause cytotoxicity.

The IC_{50} for compounds **5af, 5bf,** and heptyl(phenyl)tellane was determined using a MTT reduction assay.[32] IC_{50} values were calculated using the non-linear regression test in GraphPad Prism 7.04 using the growth inhibition rate (%) at 24 and 48 h. **5af** and **5bf** derivatives displayed cytotoxicity for the 5637 cell line in low concentrations (Table 3). These results demonstrate chalcogenobiotin derivatives are promising candidates for antitumor drugs for bladder cancer.

2.6. Cell cycle analysis

Tellurobiotin derivatives are organic molecules that reduce cell growth in a dose dependent manner by increasing the percentage of cells in the S (**5af**) and G2/M (**5bf**) phases of the cell cycle at concentrations of 12.5 μM (Fig. 7). The results indicate that **5af** and **5bf** interfere with important processes such as DNA replication and possibly others related to cell division. In this sense, the accumulation of cells in the S and G2/M phases of the cell cycle, are in agreement with the

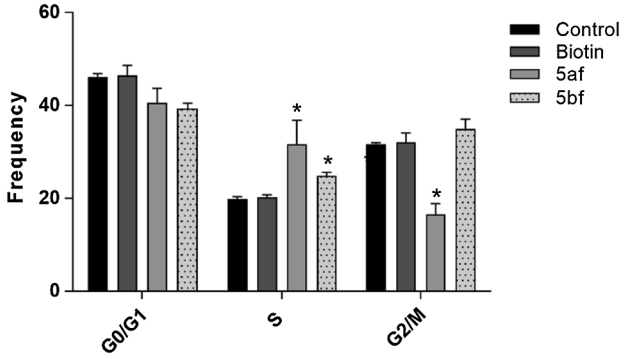

Fig. 7. Frequency of cells at each stage of the cell cycle following treatment. Untreated cells and cells treated for 24 h with **biotin**, **5af,** and **5bf** (12.5 μM) were analyzed for DNA content by flow cytometry. Each column represents a media of three independent treatments. The standard deviation of the mean is represented by an error bar. * compared to control ($p < 0.05$).

reports in the literature, in which the organotellurium AS101 presented growth stop in G2/M and the results presented by Sailer et al. 2003, show that the diphenyl ditelluride causes the cell cycle to stop at the S and G2/M phases.[33,34] Compounds containing tellurium have been used as agents/adjuvants in the treatment of some malignancies and their use is further supported by this study.[35] It has been suggested that tellurium agents can turn the oxidizing redox environment present in cancer cells into lethal reactive oxygen species which can ultimately lead to cell death via apoptosis. Normal cells largely remain unaffected because of the selective nature of this specific toxicity.[36] The use of tellurobiotin as an adjuvant and the biotin molecule as a vector may further enhance tellurium action on its own.

2.7. In silico docking study

The phosphatidylinositol 3-kinase (PI3K) family is a critical signal transduction pathway that regulates multiple cellular functions (cell growth, proliferation, differentiation, motility, and survival), and is the most frequently activated signaling pathway in human cancer, including bladder cancer.[37–39] Previous studies have indicated that PI3K inhibition represents a potential target for new anticancer agents.[37,40–42] Based on these observations, we used the molecular docking approach to predict the potential binding mode between the most active compounds in this study (**5af** and **5bf**) and the PI3Kα enzyme. The docking results indicated that both **5af** and **5bf** interact at the same site as the PI3K inhibitor PIK-93 (Fig. 8).[37] According to the docking, the **5af** and **5bf** present practically the same binding position, interacting with the Tyr864 and Asp961 residues by H-bonds, and with Met800 and Met950 by hydrophobic interactions (Fig. 8B and C). In addition, we verified that the tellurium atom interacts with the amino group from the Val879 residue backbone, similarly to PIK-93 which the nitrogen atom from the thiazole moiety makes H-bond. In both cases, nitrogen and tellurium atoms could act as H-bond acceptors (Fig. 8A). Previous crystallographic data shown that the tellurium atom, from organotellurium compounds, can interact with amino acid residues, such as the lateral chain of Pro202 (3.9 A) in a carbonic anhydrase enzyme (PDB ID 6G3R) and the carboxylic and amino group of Gly344

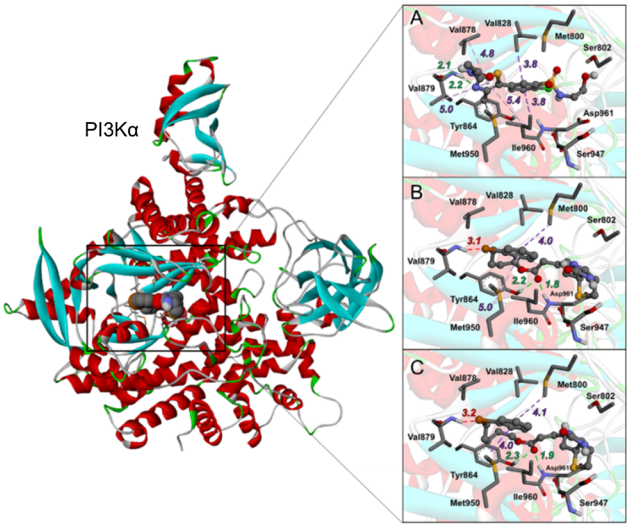

Fig. 8. Docking simulations with the PI3Kα enzyme. (**A**) The PIK-93, (**B**) **5af,** and (**C**) **5bf** molecules interact with the PI3Kα ATP binding site. Purple and green dotted lines represent hydrophobic interactions and H-bonds, respectively. The intermolecular interaction distances are in Å. PIK-93 is a well know PI3K inhibitor and was used to validate the docking protocol and to compare the interactions with the active site. For comparison, the Val879, Tyr864, Met800, Met950, and Ile960 residues from the PI3K model are represented by Val882, Tyr867, Met804, Met953, and Ile963 in the PDB ID 2CHZ structure, respectively.

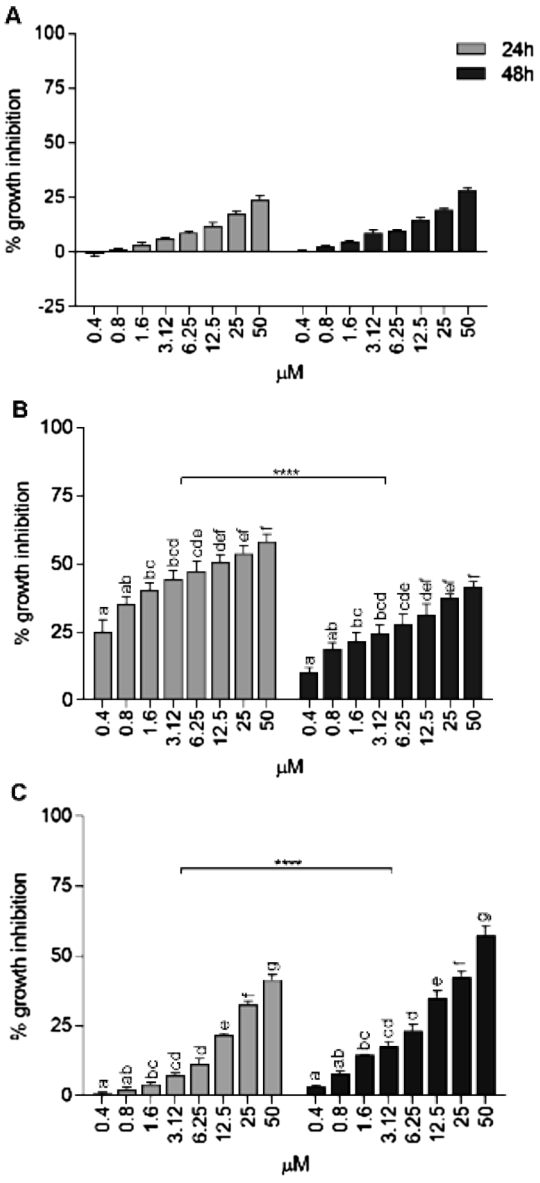

Fig. 9. Antiproliferative effect of Chalcogenobiotin derivatives investigated by MTT assay. Growth inhibition of CHO-K1 cells following exposure to **biotin** (**A**), **heptyl(phenyl)tellane** (**B**) and **5af** (**C**) after 24 and 48 h. Data are expressed as means ± SEM from three independent experiments. The letters indicate the differences between concentrations within each time. Each letter corresponds to a concentration (e.g. 0.4 μM–letter a). **** $p < 0.0001$ correspond to the difference between times 24 and 48 h.

and His269 residues (3.1–3.8 A), respectively, from sarcosine oxidase (PDB ID 1EL7).[43,44] The predicted binding energy (ΔG_{bind}) indicated that both compounds bind spontaneously with the enzyme (ΔG_{bind}: PIK-93 = −7.7 kcal/mol; **5af** = −7.0 kcal/mol; **5bf** = −7.3 kcal/mol). Together, these data support the hypothesis that **5af** and **5bf** are potential PI3K inhibitors.

2.8. In vitro toxicity

As described, the use of biotin represents an interesting strategy to increase targeted delivery of new drugs to tumor cells and reduce the cytotoxic effects of drug candidates on healthy cells. Thus, the **5af** and **5bf** derivatives as well as the biotin and heptyl(phenyl)tellane compounds were selected for testing of cytotoxicity in Chinese Hamster Ovary Cells (CHO-K1) (Fig. 9 and Table 4). CHO-K1 cells were exposed

Table 4
Susceptibility of Chinese Hamster Ovary Cells to chalcogenobiotin derivatives.[a]

Compound	IC_{50} 24 h	IC_{50} 48 h
5af	70.02 ± 9.47	34.19 ± 5.39
Heptyl(phenyl)tellane	–	–

[a] IC_{50} values are given in μM. All data were obtained from three independent experiments and are presented as mean ± SEM inhibition. Due to the noisy and incomplete data obtained for heptyl(phenyl)tellane, which reduces the ability of nonlinear regression methods to provide scientifically meaningful results, it was not possible to calculate the IC_{50} of heptyl(phenyl)tellane.

to concentrations ranged from 0.4 to 50 μM for 24 and 48 h. While biotin did not display cytotoxicity against CHO-K1 cells (Fig. 9A), heptyl(phenyl)tellane inhibited 50% of cell growth at a concentration of 12.5 μM for 24 h (Fig. 9B and Table 4).

The tellurobiotin derivatives **5af** and **5bf** demonstrated reduced cytotoxicity for CHO-K1 compared to 5637 cells (Fig. 5G–H), with compound **5af** displaying an IC_{50} of 70 μM for CHO-K1 cells (Table 4) compared to an IC_{50} of 5.8 μM for 5637 cells (Table 3).

Heptyl(phenyl)tellane displayed similar cytotoxicity against CHO-K1 cells and bladder carcinoma cells. Therefore, the introduction of tellurophenyl moiety in a biotin nucleus allowed for tuning of the toxicity rates of this nucleus for healthy and cancerous cells, improving the targeting of these new drugs candidates.

2.9. Cell viability

Similarly, the cytotoxic effect of drug candidates **5af** and **5bf** on health human leukocytes has also been tested through cell viability.[45,46] For this assay, human leukocytes were exposed to DMSO (vehicle), **5af** and **5bf** derivatives (100 μM), and *t*-butyl hydroperoxide (1 mM - positive control) for 3 h (Fig. 10). *t*-Butyl hydroperoxide caused a significant decrease in cell viability. On the other hand, incubation with **5af** and **5bf** derivatives did not present a cytotoxic effect against human leukocytes.

2.10. In vivo toxicity

As **5af** and **5bf** derivative compounds showed antitumoral activity and were not toxic to two different types of healthy cells, it was decided to test it in a more complex experimental model. Being the **5af** derivative most efficient as an antitumor agent, *in vivo* toxicity studies using Swiss male mice was performed with this compound. In this test, mice (n = 4 per group) were injected subcutaneously (s.c.) with **5af** derivative (100 μmol/kg body weight) or DMSO (1 mL/kg body weight) and observed for 7 days (168 h). Compound **5af** did not alter percent survival, as well as, dit not induce overt signs of toxicity during the observation period (see SI file, Figs. S1 and S2).

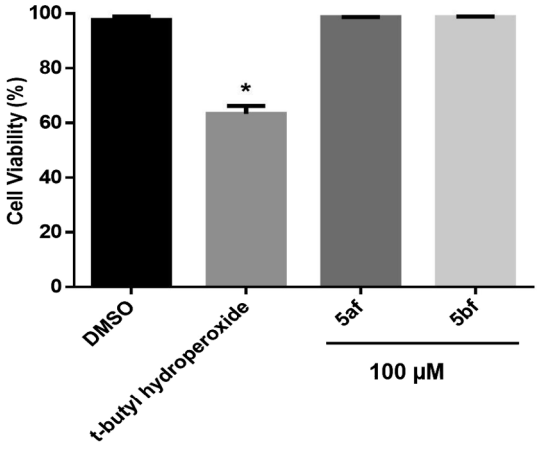

Fig. 10. Effect of chalcogenobiotin derivative compounds on human leukocyte viability *in vitro*. *t*-butyl hidroperoxide (1 mM) was used as positive control. Data are expressed as means ± S.E.M. from three independent experiments and differences are considered significant at $p < 0.05$. * ≠ DMSO (post hoc test: Tukey $p < 0.05$).

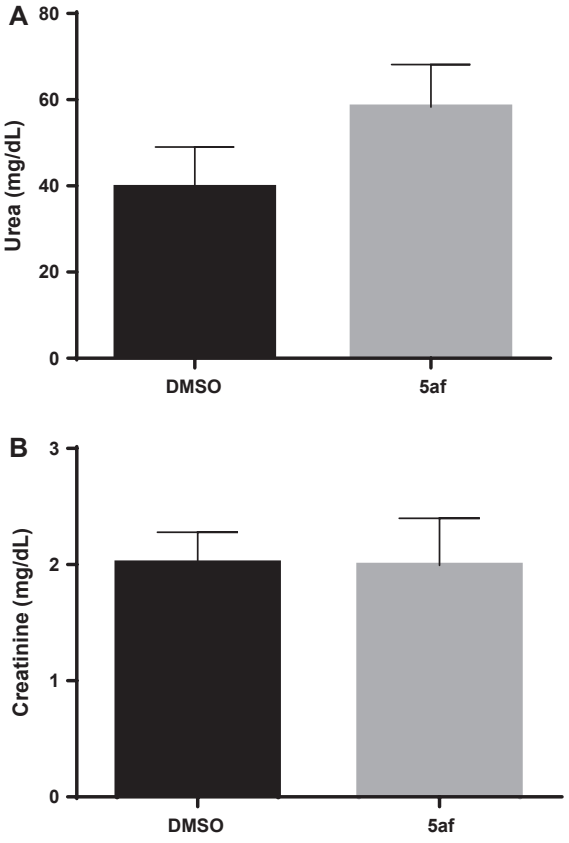

Fig. 11. Effect of **5af** (100 μmol/kg, s.c.) on urea (**A**) and (**B**) creatinine plasma levels. Data were analyzed by unpaired *t* test. There was no significant difference between groups.

Renal function markers, such as urea and creatinine in blood plasma levels were evaluated. **5af** derivative did not alter these parameters after 7 days of treatment (168 h) indicating no renal toxicity (Fig. 11).

Biomarkers of liver function were also evaluated (Fig. 12). Compound **5af** derivative altered aspartate aminotransferase (AST) (Fig. 12A), but not alanine aminotransferase (ALT) (Fig. 12B) and alkaline phosphatase activity (Fig. 12C). Increased activity of one of the three hepatic markers suggests minimal hepatotoxicity of **5af**.[47,48]

Additionally, evaluations for locomotor and exploratory behavior as well as for organ-to-body weight ratio (brain, liver, kidneys, and spleen) were also evaluated (see SI file).

3. Conclusions

The synthesis of new chalcogenobiotin derivatives using simple two-step reactions and their application as antioxidant and antitumoral agents against bladder carcinoma 5637 cells was demonstrated. The selected compounds demonstrated both antioxidant and antitumoral activity. Additionally, *in vitro* and *in vivo* toxicity was evaluated and the effective compounds did not show signs of toxicity in the performed assays.

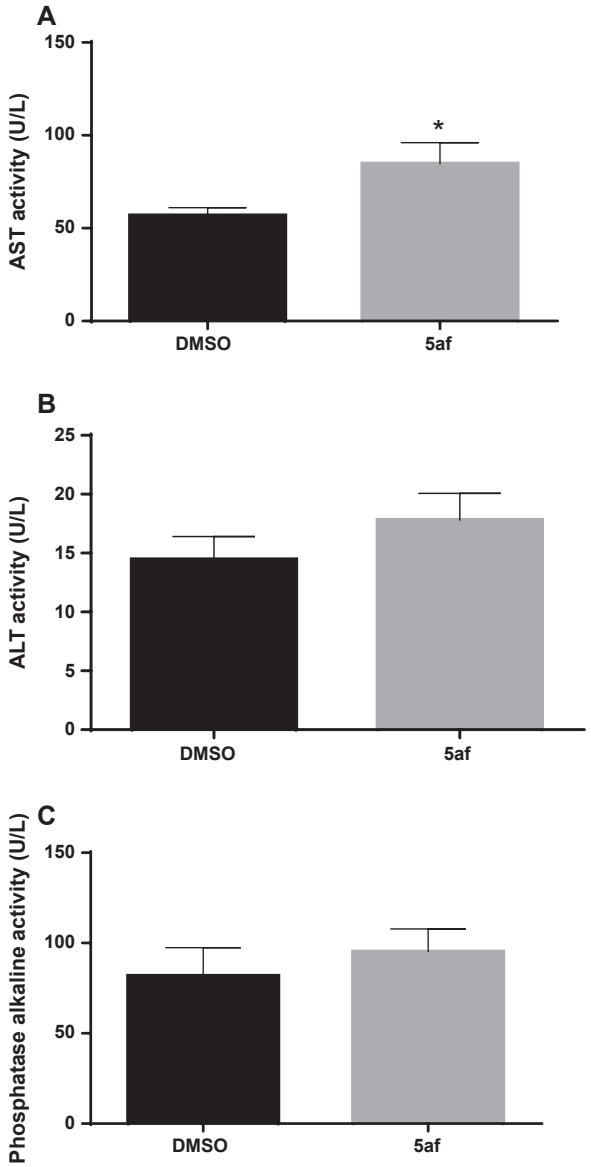

Fig. 12. Effects of **5af** (100 μmol/kg, s.c.) in AST (**A**), ALT (**B**) and alkaline phosphatase activity (**C**). Data were analyzed by unpaired *t* test. There was no significant difference between groups.

4. Experimental section

4.1. Chemistry

All reactions were run under an atmosphere of dry nitrogen or argon unless otherwise noted. DMSO, Thiobarbituric Acid (TBA), and Malondialdehyde was obtained from Sigma (St. Louis, MO). All other chemicals were of analytical grade and obtained from standard commercial suppliers. The NMR spectra were recorded with a Bruker DPX-400 spectrometer with chemical shifts expressed in parts per million (in $CDCl_3$ and Me_4Si as internal standard). Data are reported as follows: chemical shift, multiplicity (s = singlet, d = doublet, t = triplet, q = quartet, brs = broad singlet, m = multiplet), coupling constants, and number of protons. All test compounds showed > 95% purity as determined by LC-MS. LC-MS used the follows conditions: Shimadzu LC-20AD pump, Shimadzu SIL-20A autosampler, Shimadzu CTO-20A column oven (40 °C), Shimadzu SPD-M20A DAD Detector. Column: Phenomenex ref. 00F-4252-E0, Luna C18(2)5u, 5 μm, 100 Å, 4.6 mm × 150 mm. Gradient: 20–100% acetonitrile in water containing 0.01% of formic acid, Flow: 0.7 mL/min. MS: MicrOTOF QII Brucker, with ESI-source.

4.2. Synthetic procedures:

4.2.1. Preparation of bromobiotinyl derivatives 3

*4.2.1.1. Preparation of 4-Bromobutyl 5-{(1R,5S,6S)-3-oxo-7-thia-2.4-diazabicyclo[3.3.0]oct-6-yl}valerate (**3a**).* In a two-necked rounded bottom flask under argon atmosphere, fitted with a reflux condenser and magnetic stirring, biotin (4.08 mmol, 1.0 g), 1,4-dibromobutane (12.86 mmol, 1.52 mL), and DBU (12.40 mmol, 1, 85 mL) were dissolved in acetonitrile (100 mL). The reaction mixture was heated to reflux while stirring for 3 h. The solvent was then evaporated under reduced pressure. The resulting white solid was purified by column chromatography on silica gel using ethyl acetate and methanol (90:10) as eluents to give the desired product 3a. The solvent was removed on a rotary evaporator and then the product was dried under vacuum pump, resulting in a 55% yield for compound 3a; Physical state: white solid; Yield: 55%; M.P.: 80.7–84.5 °C; ^{1}H NMR (400 MHZ, $CDCl_3$) δ (ppm): 6.04 (s, 1H), 5.69 (s, 1H), 4.52–4.49 (m, 1H), 4.33–4.29 (m, 1H), 4.10 (t, 2H, J = 6.4 Hz), 3.44 (t, 2H, J = 6.6 Hz), 3.18–3.14 (m, 1H), 2.91 (dd, 1H, J^1 = 12.8 , J^2 = 4.8 Hz), 2.74 (d, 1H, J = 12.8 Hz), 2.34 (t, 2H, J = 7.5 Hz), 1.96–1.91 (m, 2H), 1.81–1.66 (m, 6H) 1.49–1.43 (m, 2H); ^{13}C NMR (100 MHz, $CDCl_3$) δ (ppm): 173.6, 163.8, 63.3, 61.9, 60.1, 55.4, 40.5, 33.9, 33.1, 29.3, 28.3, 28.2, 27.3, 24.7.

*4.2.1.2. Preparation of 5-Bromobutyl 5-{(1R,5S,6S)-3-oxo-7-thia-2.4-diazabicyclo[3.3.0]oct-6-yl}valerate (**3b**).* In a two-necked rounded bottom flask under argon atmosphere, fitted with a reflux condenser and magnetic stirring biotin (4.08 mmol, 1.0 g), 1,5-dibromopentane (12.86 mmol, 1.73 mL), and DBU (12.40 mmol, 1, 85 mL) was dissolved in acetonitrile (100 mL). The reaction mixture was heated to reflux while stirring for 3 h. After this period the solvent was evaporated under reduced pressure. The resulting white solid was purified by column chromatography on silica gel using ethyl acetate and methanol (90:10) as eluents to give the desired product 3a. The solvent was removed on a rotary evaporator and then the product was dried under vacuum pump, resulting in a 68% yield for compound 3b; Physical state: white solid; Yield: 68%; M.P.: 90.3–91.0 °C; ^{1}H NMR (400 MHZ, $CDCl_3$) δ (ppm): 6.06 (s, 1H), 5.72 (sl, 1H), 4.52–4.49 (m, 1H), 4.33–4.29 (m, 1H), 4.08 (t, 2H, J = 6.6 Hz), 3.44–3.40(m, 4H), 3.18–3.14 (m, 1H), 2.91 (dd, 1H, J^1 = 12.8 Hz, J^2 = 4.8 Hz), 2.74 (d, 1H, J = 12.8 Hz), 2.33 (t, 2H, J = 7.4 Hz), 1.68–1.47 (m, 10*H*), ^{13}C NMR (100 MHz, $CDCl_3$) δ (ppm): 173.6, 163.5, 64.0, 62.0, 60.2, 55.4, 40.5, 33.9, 33.4, 32.3, 28.3, 28,3; 27.8, 24.8, 24.64.

4.2.2. Synthesis of chalcogenobiotinyl derivatives

*4.2.2.1. Preparation of compounds **5a(a-g)** and **5b(a-g)**.* In a two-necked rounded bottom flask under argon atmosphere and magnetic stirring, diorganoyl diselenide (0.5 mmol) solubilized in 9 mL of THF, $NaBH_4$ (2.5 mmol, 0,095 g), and 3 mL of ethanol were combined. The reaction was stirred until chalcogenolate formed (colorless solution). Subsequently, biotinyl bromoalkyl ester 3 (1 mmol) dissolved in 10 mL of THF was added and the resulting mixture was stirred for 6 h. The reaction was then washed with an aqueous NH_4Cl saturated solution (3 × 20 mL) and ethyl acetate. The organic phase was dried over $MgSO_4$ and removed by filtration and by heating under reduced pressure. The compounds **5a(a-g)** and **5b(a-g)** were purified by chromatographic column on silica gel using ethyl acetate and methanol as eluents.

*4.2.2.1.1. Synthesis of 4-(phenylseleno)butyl 5-{(1R,5S,6S)-3-oxo-7-thia-2.4-diazabicyclo[3.3.0]oct-6-yl}valerate (**5aa**).* Physical state: pasty beige solid; Yield: 90%; ^{1}H NMR (400 MHZ, $CDCl_3$) δ (ppm): 7.49–7.47 (m, 2H), 7.26–7.24 (m, 3H), 5.78 (s, 1H), 5.39 (s, 1H), 4.50–4.47 (m, 1H), 4.30–4.28 (m, 1H), 4.10–4.05 (m, 2H), 3.16–3.12 (m, 1H), 2.93–2.88 (m, 3H), 2.72 (d, J = 12.8 Hz. 1H), 2.30 (t, J = 7.4 Hz.

2H), 1.76–1.61 (m, 8H), 1.47–1.39 (m, 2H); ^{13}C NMR (100 MHz, $CDCl_3$) δ (ppm): 173.4, 163.9, 132.4, 130.0, 128.9, 126.7, 63.5, 61.9, 60.0, 55.3, 40.3, 33.8, 28.5, 28.2, 28.1, 27.1, 26.4, 24.6; HRMS (TOF MS ESI+) *m/z* calcd for $C_{20}H_{28}N_2O_3SSe$ [(M + H)$^+$]: 457.1064; found: 457.1100.

4.2.2.1.2. Synthesis of 4-(4-methoxyphenylseleno)butyl 5-{(1R,5S,6S)-3-oxo-7-thia-2.4-diazabicyclo[3.3.0]oct-6-yl}valerate ***(5ab)***. Physical state: pasty yellow solid; Yield: 82%; ^{1}H NMR (400 MHZ, $CDCl_3$) δ (ppm): 7.44 (d, *J* = 8.8 Hz. 2H), 6.80 (d, *J* = 8.8 Hz. 2H), 6.27 (s, 1H), 6.02 (s, 1H), 4.48–4.45 (m, 1H), 4.29–4.25 (m, 1H), 4.04 (t, *J* = 6.0 Hz. 2H), 3.78 (s, 3H), 3.15–3.10 (m, 1H), 2.86 (d, *J* = 4.8 Hz. 1H), 2.81 (t, *J* = 6.8 Hz. 2H), 2.72 (d, *J* = 12.8 Hz. 1H), 2.29 (t, *J* = 7.68 Hz, 2H*)*, 1.72–1.61 (m, 8H), 1.46–1.40 (m, 2H); ^{13}C NMR (100 MHz, $CDCl_3$) δ (ppm): 173.4, 163.9, 159.1, 135.4, 119.6, 114.6, 63.5, 61.8, 59.9, 55.3, 55.1, 40.3, 33.7, 28.4, 28.2, 28.1, 28.0, 26.4, 24.6; HRMS (TOF MS ESI+) *m/z* calcd for $C_{21}H_{30}N_2O_4SSe$ [(M + H)$^+$]: 487.1170; found: 487.1202.

4.2.2.1.3. Synthesis of 4-(4-chlorophenylseleno)butyl 5-{(1R,5S,6S)-3-oxo-7-thia-2.4-diazabicyclo[3.3.0]oct-6-yl}valerate ***(5ac)***. Physical state: pasty yellow solid; Yield: 73%; ^{1}H NMR (400 MHZ, $CDCl_3$) δ (ppm): 7.40 (d, *J* = 8.8 Hz. 2H), 7.22 (d, *J* = 8.8 Hz. 2H), 6.35 (s, 1H), 6.11 (s, 1H), 4.49–4.46 (m, 1H), 4.29–4.26 (m, 1H), 4.06–4.04 (m, 2H), 3.15–3.11 (m, 1H), 2.91–2.86 (m, 3H), 2.73 (d, *J* = 12.8 Hz. 1H), 2.30 (t, *J* = 7.6 Hz. 2H), 1.75–1.63 (m, 8H), 1.46–1.40 (m, 2H). ^{13}C NMR (100 MHz, $CDCl_3$) δ (ppm): 173.5, 163.9, 133.8, 132.8, 129.0, 128.2, 63.4, 61.8, 60.0, 55.4, 40.4, 33.8, 28.5, 28.2, 28.1, 27.5, 26.3, 24.6; HRMS (TOF MS ESI+) *m/z* calcd for $C_{20}H_{27}ClN_2O_3SSe$ [(M + H)$^+$]: 491.0674; found: 491.0706.

4.2.2.1.4. Synthesis of 4-(4-toluylseleno)butyl 5-{(1R,5S,6S)-3-oxo-7-thia-2.4-diazabicyclo[3.3.0]oct-6-yl}valerate ***(5ad)***. Physical state: pasty beige solid; Yield: 81%; ^{1}H NMR ($CDCl_3$, 400 MHz) δ = 7.38 (d. *J* = 8 Hz. 2H), 7.07 (d, *J* = 8 Hz. 2H), 5.94 (s, 1H), 5.57 (s, 1H), 4.50–4.47 (m, 1H), 4.30–4.28 (m, 1H), 4.06–4.03 (m, 2H), 3.16–3.12 (m, 1H), 2.92–2.85 (m, 3H), 2.73 (d, *J* = 12.8 Hz. 1H), 2.31–2.28 (m, 5H), 1.74–1.65 (m, 8H), 1.46–1.41 (m, 2H); ^{13}C NMR (100 MHz, $CDCl_3$) δ (ppm): 173.6, 163.7, 136.9, 133.2, 129.8, 126.1, 63.7, 61.9, 60.1, 55.4, 40.5, 33.9, 28.6, 28.3, 28.2, 27.6, 26.6, 24.7, 21.0; HRMS (TOF MS ESI+) *m/z* calcd for $C_{21}H_{30}N_2O_3SSe$ [(M + H)$^+$]: 471.1221; found: 471.1225.

Synthesis of 4-(butylselanyll)butyl 5-{(1R,5S,6S)-3-oxo-7-thia-2.4-diazabicyclo[3.3.0]oct-6-yl}valerate ***(5ae)***: Physical state: pasty white solid; Yield: 78%; ^{1}H NMR (400 MHZ, $CDCl_3$) δ (ppm): 6.36–6.34 (m, 1H), 6.12–6.09 (m, 1H), 4.51–4.48 (m, 1H), 4.31–4.28 (m, 1H), 4.07–4.06 (m, 2H), 3.17–3.13 (m, 1H), 2.92–2.87 (m, 1H), 2.74 (d, *J* = 12.8 Hz. 1H), 2.58–2.54 (m, 4H), 2.32 (t, *J* = 7.4 Hz. 2H), 1.73–1.60 (m, 10*H*), 1.47–1.37 (m, 4H), 0.91 (t, *J* = 7.4 Hz. 3H); ^{13}C NMR (100 MHz, $CDCl_3$) δ (ppm): 173.5, 163.9, 63.6, 61.8, 59.9, 55.3, 40.3, 33.7, 32.5, 28.6, 28.2, 28.0, 26.8, 24.6, 23.5, 23.0, 22.8, 13.4; HRMS (TOF MS ESI+) *m/z* calcd for $C_{18}H_{32}N_2O_3SSe$ [(M + H)$^+$]: 437.1377; found: 437.1405.

4.2.2.1.5. Synthesis of 4-(phenyltelluro)butyl 5-{(1R,5S,6S)-3-oxo-7-thia-2.4-diazabicyclo[3.3.0]oct-6-yl}valerate ***(5af)***. Physical state: pasty yellow solid; Yield: 66%; ^{1}H NMR (400 MHZ, $CDCl_3$) δ (ppm): 7.73–7.70 (m, 2H), 7.30–7.17 (m, 3H), 5.83 (sl. 1H), 5.47 (sl. 1H), 4.50–4.47 (m, 1H), 4.31–4.27 (m, 1H), 4.05 (t, *J* = 6.4 Hz. 2H), 3.17–3.12 (m, 1H), 2.92–2.88 (m, 3H), 2.73 (d, *J* = 12.8 Hz. 1H), 2.29 (t, *J* = 7.4 Hz. 2H), 1.87–1.62 (m, 8H), 1.47–1.38 (m, 2H). ^{13}C NMR (100 MHz, $CDCl_3$) δ (ppm): 173.6, 163.6, 138.4, 129.2, 127.6, 111.5, 63.5, 61.9, 60.1, 55.4, 40.5, 33.9, 30.8, 28.3, 28.2, 24.8, 7.7; HRMS (TOF MS ESI+) *m/z* calcd for $C_{20}H_{28}N_2O_3STe$ [(M + H)$^+$]: 507.0961; found 507.0995.

4.2.2.1.6. Synthesis of 4-(phenylthio)butyl 5-{(1R,5S,6S)-3-oxo-7-thia-2.4-diazabicyclo[3.3.0]oct-6-yl}valerate ***(5ag)***. Physical state: pasty white solid; Yield: 76%; ^{1}H NMR (400 MHZ, $CDCl_3$) δ (ppm): 7.32–7.25 (m, 4H), 7.18–7.14 (m, 1H), 6.27 (s, 1H), 5.99 (s, 1H), 4.47–4.44 (m, 1H), 4.28–4.25 (m, 1H), 4.06 (t, *J* = 6.2 Hz. 2H), 3.15–3.10 (m, 1H), 2.95–2.85 (m, 3H), 2.71 (d, *J* = 12.8 Hz. 1H), 2.30 (t, *J* = 7.4 Hz. 2H), 1.74–1.62 (m, 8H), 1.45–1.40 (m, 2H); ^{13}C NMR (100 MHz, $CDCl_3$) δ (ppm): 173.5, 163.9, 136.2, 129.0, 128.7, 125.8, 63.6, 61.8, 60.0, 55.4, 40.4, 33.8, 33.1, 28.2, 28.1, 27.5, 25.4, 24.6; HRMS (TOF MS ESI+) *m/z* calcd for $C_{20}H_{28}N_2O_3S_2$ [(M + H)$^+$]: 409.1620; found: 409.1638.

4.2.2.1.7. Synthesis of 5-(phenylseleno)pentyl 5-{(1R,5S,6S)-3-oxo-7-thia-2.4-diazabicyclo[3.3.0]oct-6-yl}valerate ***(5ba)***. Physical state: pasty beige solid; Yield: 92%; ^{1}H NMR (400 MHZ, $CDCl_3$) δ (ppm):7.47–7.45 (m, 2H), 7.28–7.20 (m, 3H), 6.25 (s, 1H), 6.03 (s, 1H), 4.46–4.43 (m, 1H), 4.27–4.26 (m, 1H), 4.08–4.01 (m, 2H), 3.14–3.10 (m, 1H), 2.91–2.84 (m, 3H), 2.71 (d, *J* = 12.8 Hz. 1H), 2.33–2.28 (m, 2H), 1.72–1.61 (m, 8H), 1.51–1.44 (m, 4H); ^{13}C NMR (100 MHz, $CDCl_3$) δ (ppm): 173.7, 164.2, 132.4, 130.5, 129.0, 126.7, 64.2, 62.1, 60.2, 55.5, 40.5, 33.9, 29.7, 28.4, 28.3, 28.1, 27.6, 26.1, 24.8; HRMS (TOF MS ESI+) *m/z* calcd for $C_{21}H_{30}N_2O_3SSe$ [(M + H)$^+$]: 471.1221; found: 471.1207.

4.2.2.1.8. Synthesis of 5-(4-methoxyphenylseleno)pentyl 5-{(1R,5S,6S)-3-oxo-7-thia-2.4-diazabicyclo[3.3.0]oct-6-yl}valerate ***(5bb)***. Physical state: pasty beige solid; Yield: 93%; ^{1}H NMR (400 MHZ, $CDCl_3$) δ (ppm): 7.44 (d, *J* = 8.6 Hz. 2H), 6.80 (d, *J* = 8.6 Hz. 2H), 6.17 (s, 1H), 5.90 (s, 1H), 4.48–4.45 (m, 1H), 4.29–4.26 (m, 1H), 4.03 (t, *J* = 6.6 Hz. 2H), 3.78 (s, 3H), 3.16–3.12 (m, 1H), 2.90–2.86 (m, 1H), 2.80 (t, *J* = 7.4 Hz. 2H), 2.72 (d, *J* = 12.8 Hz. 1H), 2.30 (t, *J* = 7.4 Hz. 2H), 1.71–1.58 (m, 8H), 1.48–1.40 (m, 4H); ^{13}C NMR (100 MHz, $CDCl_3$) δ (ppm): 173.5, 163.9, 159.1, 135.3, 119.9, 114.6, 63.9, 61.9, 60.0, 55.3, 55.1, 40.3, 33.8, 29.6, 28.6, 28.2, 28.1, 27.9, 25.9, 24.6; HRMS (TOF MS ESI+) *m/z* calcd for $C_{22}H_{32}N_2O_4SSe$ [(M + H)$^+$]: 501.1326; found: 501.1340.

4.2.2.1.9. Synthesis of 5-(4-chlorophenylseleno)pentyl 5-{(1R,5S,6S)-3-oxo-7-thia-2.4-diazabicyclo[3.3.0]oct-6-yl}valerate ***(5bc)***. Physical state: pasty white sold; Yield: 80%; ^{1}H NMR (400 MHZ, $CDCl_3$) δ (ppm): 7.40 (d, *J* = 8.4 Hz. 2H), 7.22 (d, *J* = 8.4 Hz. 2H), 5.67 (s, 1H), 5.32 (s, 1H), 4.51–4.47 (m, 1H), 4.31–4.28 (m, 1H), 4.04 (t, *J* = 6.6 Hz. 2H), 3.17–3.12 (m, 1H), 2.92–2.87 (m, 3H), 2.73 (d, *J* = 12.8 Hz. 1H), 2.31 (t, *J* = 7.4 Hz. 2H), 1.73–1.60 (m, 8H), 1.49–1.42 (m, 4H); ^{13}C NMR (100 MHz, $CDCl_3$) δ (ppm): 173.7, 163.5, 133.9, 132.9, 129.2, 128.5, 64.2, 61.9, 60.1, 55.4, 40.5, 33.9, 29.6, 28.3, 28.2, 28.1, 28.0, 26.1, 24.8; HRMS (TOF MS ESI+) *m/z* calcd for $C_{21}H_{29}ClN_2O_3SSe$ [(M + H)$^+$]: 505.0831; found: 505.0861.

4.2.2.1.10. Synthesis of 5-(4-toluylseleno)pentyl 5-{(1R,5S,6S)-3-oxo-7-thia-2.4-diazabicyclo[3.3.0]oct-6-yl}valerate ***(5bd)***. Physical state: pasty white solid; Yield: 92%; ^{1}H NMR (400 MHZ, $CDCl_3$) δ (ppm): 7.38 (d, *J* = 8.2 Hz. 2H), 7.06 (d, *J* = 8.2 Hz. 2H), 4.52–4.49 (m, 1H), 4.33–4.30 (m, 1H), 4.04 (t, *J* = 6.6 Hz. 2H), 3.18–3.13 (m, 1H), 2.93–2.84 (m, 3H), 2.74 (d, *J* = 12.8 Hz.1H), 2.33–2.29 (m, 5H), 1.73–1.60 (m, 8H), 1.49–1.42 (m, 4H); ^{13}C NMR ($CDCl_3$, 100 MHz) δ (ppm): 173.6, 163.4, 136.8, 133.1, 129.8, 126.4, 64.3, 62.1, 60.3, 55.3, 40.5, 33.9, 29.8, 28.4, 28.3, 28.1, 28.0, 26.1, 24.8, 21.0; HRMS (TOF MS ESI+) *m/z* calcd for $C_{22}H_{32}N_2O_3SSe$ [(M + Na)$^+$]: 507.1197; found: 507.1205.

4.2.2.1.11. Synthesis of 5-(butylselanyll)pentyl 5-{(1R,5S,6S)-3-oxo-7-thia-2.4-diazabicyclo[3.3.0]oct-6-yl}valerate ***(5be)***. Physical state: pasty white solid; Yield: 78%; ^{1}H NMR (400 MHZ, $CDCl_3$) δ (ppm): 6.22 (s, 1H), 5,90 (sl. 1H), 4.51–4.48 (m, 1H), 4.32–4.29 (m, 1H), 4.06 (t, *J* = 6.8 Hz. 2H), 3.18–3.13 (m, 1H), 2.90 (dd, J^1 = 12.6 Hz. J^2 = 5.0 Hz. 1H), 2.74 (d, *J* = 12.8 Hz. 1H), 2.55 (t, *J* = 7.4 Hz. 4H), 2.33 (t, *J* = 7.4 Hz. 2H), 1.72–1.60 (m, 10*H*), 1.48–1.37 (m, 6H), 0.91 (t, *J* = 7.4 Hz. 3H); ^{13}C NMR (100 MHz, $CDCl_3$) δ (ppm): 173.6, 163.9, 64.1, 61.9, 60.1, 55.4, 40.4, 33.8, 32.6, 30.1, 28.3, 28.1, 28.0, 26.2, 24.7, 23.6, 23.5, 22.9, 13.5; HRMS (TOF MS ESI+) *m/z* calcd for $C_{19}H_{34}N_2O_3SSe$ [(M + H)$^+$]: 451.1534; found: 451.1518.

4.2.2.1.12. Synthesis of 5-(phenyltelluro)pentyl 5-{(1R,5S,6S)-3-oxo-7-thia-2.4-diazabicyclo[3.3.0]oct-6-yl}valerate ***(5bf)***. Physical state: pasty yellow solid; Yield: 68%; ^{1}H NMR (400 MHZ, $CDCl_3$) δ (ppm): 7.70–7.68 (m, 2H), 7.30–7.16 (m, 3H), 6.28 (s, 1H), 6.04 (s, 1H), 4.47–4.43 (m, 1H), 4.28–4.25 (m, 1H), 4.02 (t, *J* = 6.6 Hz. 2H),

3.15–3.10 (m, 1H), 2.90–2.84 (m, 3H), 2.71 (d, J = 12.8 Hz. 1H), 2.30 (t, J = 7.4 Hz. 2H), 1.75–1.57 (m, 8H), 1.46–1.39 (m, 4H); ^{13}C NMR (100 MHz, $CDCl_3$) δ (ppm): 173.5, 163.9, 138.0, 128.9, 127.3, 111.5, 63.9, 61.8, 59.9, 55.3, 40.3, 33.8, 31.1, 28.2, 28.1, 28.0, 27.8, 24.6, 8.1; HRMS (TOF MS ESI+) m/z calcd for $C_{21}H_{30}N_2O_3STe$ [$(M + Na)^+$]: 543.0937; found: 543.0967.

*4.2.2.1.13. Synthesis of 5-(phenylthio)pentyl 5-{(1R,5S,6S)-3-oxo-7-thia-2.4-diazabicyclo[3.3.0]oct-6-yl}valerate (**5bg**).* Physical state: pasty white solid; Yield: 79%; ^{1}H NMR (400 MHZ, $CDCl_3$) δ (ppm): 7.32–7.24 (m, 4H), 7.16–7.13 (m,1H), 6.20 (s, 1H), 5.95 (s, 1H), 4.46–4.43 (m, 1H), 4.27–4.24 (m, 1H), 4.04 (t, J = 6.4 Hz. 2H), 3.15–3.10 (m, 1H), 2.93–2.84 (m, 3H), 2.72 (d, J = 12.8 Hz. 1H), 2.30 (t, J = 7.4 Hz. 2H), 1.70–1.61 (m, 8H), 1.52–1.41 (m, 4H); ^{13}C NMR ($CDCl_3$, 100 MHz) δ = 173.5, 163.9, 136.6, 128.9, 128.7, 125.6, 63.9, 61.9, 60.0, 55.3, 40.3, 33.8, 33.3, 28.6, 28.2, 28.1, 28.0, 24.9, 24.6; HRMS (TOF MS ESI +) m/z calcd for $C_{21}H_{30}N_2O_3S_2$ [$(M + H)^+$]: 423.1776; found: 423.1783.

4.3. Antioxidant studies

4.3.1. DPPH radical scavenging assay

Analysis was performed as previously described by Pereira et al (2014).[24] Biotin derivative compounds (1 mM) were mixed with 0.3 mM DPPH in ethanol. A time curve was made for the 5af and 5bf compounds (final concentrations 500 μM). Absorbance was read at 518 nm every 30 min for 180 min. BHT (final concentration 500 μM) and diphenyl diselenide (final concentration 2 mM) were used as positive controls.

4.3.2. Thiobarbituric acid reactive substances (TBARS)

Analysis was performed as previously described by Ohkawa et al (1979).[27] The incubation system to induce lipid peroxidation consisted of phosphatidylcholine (0.4 mg), iron sulfate (55 μM), Tris-HCl buffer pH 7.4 (1.85 mM), and biotin derivatives (final concentration 0–200 μM). The system was incubated for 30 min at 37 °C. Afterward, acetic acid buffer pH 3.4 and thiobarbituric acid (0.22%) were added and the samples were then incubated for one hour at 100 °C. To extract the thiobarbituric acid reactive substances (pink color) 400 μL of *N*-butanol was added. Then, the tubes were stirred for 30 s and centrifuged for 10 min at 6000 rpm. The supernatant was read at 532 nm. A MDA curve was prepared as a standard. Diphenyl diselenide (0–400 μM) and α-tocopherol (0–200 μM) were tested as positive control. The biotin derivative compounds were dissolved in DMSO.

4.3.3. Thiol peroxidase-like activity

Analysis was performed as previously described by Iwaoka and Tomoda (1994)[28] with few modifications. This method determines whether the derivatives of biotin can mimic the enzyme glutathione peroxidase activity (GPx). Thiophenol was used as an alternative to glutathione. The incubation system consisted of ethanol, thiophenol (2.5 mM), DMSO (blank) or compounds (final concentration of 0–450 μM), and hydrogen peroxide (2.3 mM). Ebselen and Diphenyl diselenide (55 μM) were used as a positive control. The reaction was monitored spectrofotometricaly at 305 nm for 20 min.

4.4. Antitumoral studies

4.4.1. Cell culture

Human bladder carcinoma cells (line 5637) were obtained from the bank of the Rio de Janeiro cells (PABCAM, Federal University of Rio de Janeiro, RJ, Brazil) and cultured in *DMEM* medium (Vitrocell Embriolife, Brasil) supplemented with 10% fetal bovine serum (Gibco, USA) in a humidified incubator at 37 °C with 5% CO_2 and 95% air. All experiments were performed with cells in its logarithmic growth phase.

4.4.2. MTT cell proliferation and cytotoxicity assay

The viability of 5637 cells was determined by measuring the reduction of MTT (3-[4,5-dimethyl-thiazol-2-il]-2,5-diphenyltetrazolium bromide) to formazan crystals.[1] Briefly, 5637 cells seeded at a density of 2×10^4 cells per well in 96 well plates were cultured for 24 h in ideal conditions. The medium was then aspirated and replaced by an equal volume (100 μL per well) DMEM/FBS containing different concentrations of the conditioning chalcogenobiotin derivatives (0.4–100 μM). In controls wells 100 μL DMEM/FBS were added, and vehicle controls were added with a corresponding DMSO concentration used in the dilution of the stock concentration of the test substance (DMSO concentration did not exceeded 0.5%). Following the above treatments, MTT at 5 mg/mL in phosphate-buffered saline (PBS) was added to each well, and the cells were incubated at 37 °C for an additional 3 h. The supernatant was discarded, and 150 μL of dimethyl sulfoxide was added to each well for 10 min to dissolve the formazan crystals. The optical density levels of the cell cultures were measured spectrophotometrically using a dual beam microplate reader (Thermo-TP Plate Reader) at 492 nm. The inhibition (%) of cell proliferation was determined as follows: growth inhibition rate (%) = $[1 - (Abs492_{treated\ cells}/Abs492_{control\ cells})] \times 100$.

4.4.3. Cell cycle assay with PI

The evaluation of DNA content of cell strain 5637 after 24 h treatment with the compounds **5af** and **5bf** (concentration 12,5 μM) was based on the use of fluorescent DNA intercalator, propidium iodide (PI). The detection was performed in a Guava® Flow Cytometry easyCyte™ System plus flow cytometer. Cell cycle evaluations were performed according to the manufacturer's protocol using the Guava® Cell Cycle (Merck KGaA) reagent kit.

4.4.4. Data analysis

Data sets from MTT were analyzed using two-way ANOVA followed by Tukey's test for multiple comparisons. Cell cycle distribution was analyzed by two-way ANOVA followed by T-test for multiple comparisons. $p < 0.05$ was considered significant for all analyses. All data were expressed as mean ± SEM of triplicates.

4.5. Cell viability

Analysis was performed as previously described by Bueno et al. (2013).[49] Heparinized venous blood was obtained from healthy donors. The protocol was approved by the Ethical Committee of UFSM (n. 089.0.243.000–07). Isolated leukocytes (2×10^6/mL) were incubated for 3 h with DMSO (0.5%), 1 mM *t*-butyl hidroperoxide (positive control), or indicated compounds (100 μM) in a Hank's buffer solution containing 10% human plasma. Cell viability were determined by Trypan blue exclusion.

4.6. In vivo study

All experiments were performed in accordance with Law 11.794, of October 8, 2008, Decree 6899, of July 15, 2009, with the rules issued by the National Council for Control of Animal Experimentation (CONCEA), and was approved by the Ethic Committee on Animal Use of the Federal University of Santa Maria (CEUA/UFSM) in the meeting of 03/31/2016 (Protocol number CEUA 4622031115).

4.6.1. Treatment

The toxicity study was conducted using adults Swiss male mice (25–30 g). Animals were randomized in two groups (n = 4 per group), and DMSO (1 mL/kg of body weight) or 5af (100 μmol/kg of body weight) were subcutaneously administered. Mice were monitored by a closed circuit TV for 168 h after the injection. Body weight, food, and water intake were evaluated daily. After seven days, mice were euthanized by decapitation and the blood and organs were collected.

The markers of kidney (urea and creatinine) and liver (aspartate aminotransferase (AST) and alanine aminotransferase (ALT)) function were analysed in serum using commercial kits (Labtest Diagnostica SA, Lagoa Santa, Minas Gerais, Brazil).

4.7. Data analysis

The *in vitro* analyses were repeated three times. Data were analyzed using one or two-way ANOVA, followed by Tukey test. The difference was considered to be significant when $p < 0.05$. Regarding the *in vivo* study, the data were analyzed using Log-rank (Mantel-Cox) test for analysis of survival and the unpaired *t* test for biochemical analysis. The difference was considered to be significant when $p < 0.05$. Data analysis was performed with the software GraphPad v. 6

5. Notes

The authors declare no competing financial interest.

Author contributions

OEDR., AL, ACFS, LD, FDG contributed in the synthesis of chalcogenobiotin derivatives; MSS, CSO, FKS, TC contributed in the antitumoral evaluation; BCP, FDS, JBTR contributed in the antioxidant and toxicity evaluation; PAN contributed in the docking studies. AL and MSS contributed equally to this work.

All authors wrote and revised the manuscript.

Declaration of Competing Interest

The authors declare that they have no known competing financial interests or personal relationships that could have appeared to influence the work reported in this paper.

Acknowledgment

The authors gratefully acknowledge CAPES – Finance Code 001, CAPES-PROEX, CAPES-PRINT, CNPq (Ed. Universal 400791/2016-1, Produtividade em Pesquisa 303387/2015-7, 306240/2018-1 Pesquisador Visitante- 401397/2014-9) for financial support.

Appendix A. Supplementary material

Supplementary data to this article can be found online at https://doi.org/10.1016/j.bmc.2020.115423.

References

1. Seki M, Mori Y, Hatsuda M, Yamada S-I. A novel synthesis of (+)-biotin from L-cysteine. *J Org Chem.* 2002;67:5527–5536.
2. Hua G, Du J, Cordes DB, Slawin AMZ, Woollins JD. Efficient synthesis of novel chalcogencontaining derivatives of DNA nucleobases. *Tetrahedron.* 2015;71:1792–1798.
3. Rampon DS, Rodembusch FS, Schneider JMFM, et al. Novel selenoesters fluorescent liquid crystalline exhibiting a rich phase polymorphism. *J Mater Chem.* 2010;20:715–722.
4. Rodrigues OED, Saraiva GD, Nascimento RO, et al. Synthesis and characterization of selenium-carbon nanocables. *Nano Lett.* 2008;8:3651–3655.
5. Sartori G, Jardim NS, Sari MHM, et al. Antiviral action of diphenyl diselenide on herpes simplex virus 2 infection in female BALB/c Mice. *J Cell Biochem.* 2016;117:1638–1648.
6. Pesarico AP, Sartori G, dos Santos CFA, et al. 1,1'-Dithienyl diselenide pro-oxidant activity accounts for antibacterial and antifungal activities. *Microbiol Res.* 2013;168:563–568.
7. Leite MR, Cechella JL, Mantovani AC, Duarte MMMF, Nogueira CW, Zeni G. Swimming exercise and diphenyl diselenide-supplemented diet affect the serum levels of pro-and anti-inflammatory cytokines differently depending on the age of rats. *Cytokine.* 2015;71:119–123.
8. Rossato JI, Ketzer LA, Centurião FB, et al. Antioxidant properties of new chalcogenides against lipid peroxidation in rat brain. *Neurochem Res.* 2002;27:297–303.
9. Tabarelli G, Dornelles L, Iglesias BA, et al. Synthesis and antitumoral lung carcinoma A549 and antioxidant activity assays of new chiral β-aryl-chalcogenium azide compounds. *ChemistrySelect.* 2017;2:8423–8430.
10. de Andrade RB, Gemelli T, Guerra RB, Funchal C, Wannmacher CMD. Inhibition of creatine kinase activity by 3-butyl-1-phenyl-2-(phenyltelluro0oct-en-1-one in the cerebral cortex and cerebellum of young rats. *J Appl Toxicol.* 2010;30:611–616.
11. Nogueira CW, Rocha JBT. Diphenyl diselenide a janus-faced molecule. *J Brazil Chem Soc.* 2010;21:2055–2071.
12. Sanmartín C, Plano D, Sharma AK, Palop JA. Selenium compounds, apoptosis and other types of cell death: An overview for cancer therapy. *Int J Mol Sci.* 2012;13:9649–9672.
13. Azad GK, Tomar RS. Ebselen, a promising antioxidant drug: mechanismos of action and targets of biological pathways. *Mol Bio Rep.* 2014;41:4865–4879.
14. Heimfarth L, Ferreira FS, Pierozana P, et al. Astrocyte-neuron interaction in diphenyl ditelluride toxicity directed to the cytoskeleton. *Toxicology.* 2017;379:1–11.
15. De Souza D, Mariano DOC, Nedel F, Schultz E, Campos VF, Seixas F, da Silva RS, Munchen TS, Ilha V, Dornelles L, Braga AL, Rocha JBT, Collares T, Rodrigues OED. New organochalcogen multitarget drug: synthesis and antioxidant and antitumoral activities of chalcogenozidovudine derivatives. *J Med Chem.* 2015;58:3329–3339.
16. da Rosa RM, Piccoli BC, da Silva FD'A, Dornelles L, Rocha JBT, Sonego MS, et al. Stnthesis, antioxidant and antitumoral activites of 5'-arylchalcogeno-3-aminothymidine (ACAT) derivatives. *MEDCHEMCOMM.* 2017;8:408–414.
17. Tabayoyong WB, Kamat AM, O'Donnell MA, et al. Systematic review on the utilization of maintenance intravesical chemotherapy in the management of non-muscle-invasive bladder cancer. *Eur Urology Focus.* 2018;4:512–521.
18. Tan WS, Kelly JD. Intravesical device-assisted therapies for non-muscle-invasive bladder cancer. *Nat Rev Urol.* 2018;15:667–685.
19. Su J, Chen F, Cryns VL, Messersmith PB. Catechol polymers for pH-responsive, targeted drug delivery to cancer cells. *J Am Chem Soc.* 2011;133:11850–11853.
20. Babak MV, Plazuk D, Meier SM, et al. Half-sandwich ruthenium(II) biotin conjugates as biological vectors to cancer cells. *Chem-Eur J.* 2015;21:5110–5117.
21. Qu W, Chen W-H, Kuang Y, et al. Avidin-biotin interaction mediated peptide assemblies as efficient gene delivery vectors for cancer therapy. *Mol Pharm.* 2013;10:261–269.
22. Reddy JA, Low PS. Folate-mediated targeting of therapeutic and imaging agents to cancers. *Crit Rev Ther Drug Carrier Syst.* 1998;15:587–627.
23. Gill JG, Piskounava E, Morrison SJ. Cancer, oxidative stress, and metastasis. *Cold Spring Harb Symp.* 2016;81:163–175.
24. Pereira RP, Boligon AA, Appel AS, et al. Chemical composition, antioxidant and anticholinesterase activity of Melissa officinalis. *Ind Crop Prod.* 2014;53:34–45.
25. Kudryavtseva AV, Krasnov GS, Dmitriev AA, et al. Mitochondrial dysfunction and oxidative stress in aging and cancer. *Oncotarget.* 2016;7:44879–44905.
26. Kanno K, Wu MK, Scapa EF, Roderick SL, Cohen DE. Structure and function of phosphatidylcholine transfer protein (PC-TP)/StarD2. *Biochim Biophys Acta.* 2007;1771:654–662.
27. Ohkawa H, Ohishi N, Yagi K. Assay for lipid peroxides in animal tissues by thiobarbituric acid reaction. *Anal Biochem.* 1979;95:351–358.
28. Iwaoka M, Tomoda S. A model study on the effect of an amino group on the antioxidant activity of glutathione peroxidase. *J Am Chem Soc.* 1994;116:2557–2561.
29. Barbosa NV, Nogueira CW, Nogara PA, de Bem AF, Aschner M, Rocha JBT. Organoselenium compounds as mimics of selenoproteins and thiol modifier agents. *Metallomics.* 2017;9:1703–1734.
30. Tripodo G, Mandracchia D, Collina S, Rui M, Rossi D. New perspectives in cancer therapy: the biotin-antitumor molecule conjugates. *Med Chem.* 2014;1:1–8.
31. Plazuk D, Zakrzewski J, Salmain M, et al. Ferrocene-biotin conjugates targeting cancer cells: synthesis, interaction with avidin, ytotoxic properties and the crystal structure of the complex of avidin with a biotin-linker-ferrocene conjugate. *Organometallics.* 2013;32:5774–5783.
32. Mosmann T. Rapid colorimetric assay for cellular growth and survival: application to proliferation and cytotoxicity assays. *J Immunol Methods.* 1983;16:55–63.
33. Kalechman Y, Albeck M, Sredni B. In vivo synergistic effect of the immunomodulator AS101 and the PKC inducer bryostation. *Cell Immunol.* 1992;143:143–153.
34. Sailer BL, Liles N, Dickerson S, Chesteen TG. Cytometric determination of novel organotellurium compound toxic ity in a promyelocytic (HL-60) cell line. *Arch Toxicol.* 2003;77:30–36.
35. Jamier V, Ba LA, Jacob C. Selenium- and tellurium-containing multifunctional redox agents as biochemical redox modulators with selective cytotoxicity. *Chemistry.* 2010;16:10920–10928.
36. Hayun M, Saida H, Albeck M, Peled A, Haran-Ghera N, Sredni B. In duction therapy in a multiple myeloma mouse model using a combination of AS101 and melphalan, and the activity of AS101 in a tumor microenvironment model. *Exp Hematol.* 2009;37:593–603.
37. Knight ZA, Gonzalez B, Feldman ME, et al. A pharmacological map of the PI3-K family defines a role for p110α in insulin signaling. *Cell.* 2006;125:733–747.
38. Knowles MA, Platt FM, Ross RL, Hurst CD. Phosphatidylinositol 3-kinase (PI3K) pathway activation in bladder cancer. *Cancer Metast Rev.* 2009;28:305–316.
39. Fruman DA, Rommel C. PI3K and cancer:lessons, challenges and opportunities. *Nat Rev Drug Discov.* 2014;13:140–156.
40. Zhang C, Yang N, Yang CH, et al. S9, a novel anticancer agent, exerts its anti-proliferative activity by interfering with both PI3K-Akt-Mtor signaling and microtubule cytoskeleton. *PLoS ONE.* 2009;4:e4881.
41. Kim M-S, Kim J-E, Lim DY, et al. Naproxen induces cell cycle arrest and apoptosis in human urinary bladder cancer cell lines and chemically induced cancers by targeting PI3-K. *Cancer Prev Res.* 2014;7:236–245.
42. Janku F, Yap TA, Meric-Bernstam F. Targeting the PI3K pathway in cancer: are we making headway? *Nat Rev Clin Oncol.* 2018:15273–15291.
43. Tanini D, Ricci L, Capperucci A, et al. Synthesis of novel tellurides bearing

benzensulfonamide moiety as carbonic anhydrase inhibitors with antitumor activity. *Eur J Med Chem.* 2019;181:111586.
44. Wagner MA, Trickey P, Chen Z-W, Mathews FS, Jorns MS. Monomeric sarcosine oxidase: 1 Flavin reactivity and active site binding determinats. *Biochemistry.* 2000;39:8813–8824.
45. Bueno DC, Meinerz DF, Allebrandt J, et al. Cytotoxicity and genotoxicity evaluation of organochalcogens in human leucocytes: a comparative study between ebselen, diphenyl diselenide, and diphenyl ditelluride. *BioMed Res Int.* 2013:537279.
46. Waczuk EP, Kamdem JP, Abolaji AO, et al. Euphorbia tirucalli aqueous extract induces cytotoxicity, genotoxicity and changes in antioxidant gene expression in human leukocytes. *Toxicol Res.* 2015;4:739–748.
47. Giannini EG, Testa R, Savarino V. Liver enzyme alteration: a guide for clinicians. *CMAJ.* 2005;172:367–379.
48. Ozer J, Ratner M, Shawc M, Bailey W, Schomaker S. The current state of serum biomarkers of hepatotoxicity. *Toxicology.* 2008;245:194–205.
49. Bueno DC, Meinerz DF, Allebrandt J, et al. Cytotoxicity and genotoxicity evaluation of organochalcogens in human leucocytes: a comparative study between ebselen, diphenyl diselenide, and diphenyl ditelluride. *Bio Med Res Int.* 2013;2013:1.